Plasticity of Plant Form and Function Sustains Productivity and Dominance along Environment and Competition Gradients. A Modeling Experiment with GEMINI

Vincent Maire, Jean-Francoise Soussana, Nicolas Gross, Bruno Bachelet, Loic Pages, Raphaël Martin, Tanja Reinhold, Christian Wirth, David R.C. Hill

Running title: Plant plasticity modeling experiment

Title: Plasticity of plant form and function sustains productivity and dominance along environment and competition gradients. A modeling experiment with GEMINI.

Vincent Maire[1], Jean-François Soussana[1], Nicolas Gross[1*], Bruno Bachelet[1**], Loïc Pagès[2], Raphaël Martin[1], Tanja Reinhold[3], Christian Wirth[3***] and David Hill[4****]

[1]INRA UR874 UREP, Grassland Ecosystem Research, F-63100 Clermont-Ferrand, France

[2]INRA UR1115 PSH, Plantes et Systèmes de cultures Horticoles, F-84914 Avignon, France

[3]Max-Planck Institute for Biogeochemistry, D-07745 Jena, Germany

[4]Clermont Université, Université Blaise Pascal, LIMOS, BP 10448, F-63000 Clermont-Ferrand, France

[*] Current address: CNRS, Centre d'étude Biologique de Chizé, 79360 Beauvoir-Sur-Niort, France

[**] Current address: Clermont Université, Université Blaise Pascal, LIMOS, BP 10448, F-63000 Clermont-Ferrand, France

[***] Current address: Universität Leipzig, Institut für Biologie I, 04103 Leipzig, Germany

[****] Current address: CNRS, UMR 6158, LIMOS, F-63173 Aubière, France

Authors for correspondence (phone +33 473 62 44 23; e-mail jfsoussana@clermont.inra.fr,)

Email addresses: nicolas.gross@cebc.cnrs.fr, david.hill@univ-bpclermont.fr, bachelet@isima.fr, rmartin@clermont.inra.fr, cwirth@uni-leipzig. de

Website of GEMINI project: https://www1.clermont.inra.fr/urep/modeles/gemini.htm

Figure: 8; **Table:** 2

Key-Words: Partitioning, growth, carbon, nitrogen, functional balance, coordination theory, biodiversity; grassland community

Abstract

GEMINI, a mechanistic model linking plant functional traits, plant populations, community dynamics, and ecosystem scale fluxes in grasslands has been reported in a companion paper (Soussana et al., 2012). For monocultures and six species mixtures of perennial grass species, this model has been successfully evaluated against experimental data of above-ground net primary productivity (ANPP) and plant community structure across nitrogen and disturbance (cutting frequency) gradients. The GEMINI model combines two categories of processes: i) C and N fluxes, ii) morphogenesis and architecture of roots and shoots and demography of clonal plant axes. These two process categories constrain the form and function of the simulated clonal plants within plastic limits. We show here that the plasticity of the simulated plant populations accounts for well-established empirical laws: i) root:shoot ratio, ii) self-thinning, iii) critical shoot N content, and iv) role of plant traits (specific leaf area and plant height) for population response to environmental gradients (nitrogen and disturbance). Moreover, we show that model versions for which plasticity simulation has been partly or fully suppressed have a reduced ANPP in monocultures and in binary mixtures and do not capture anymore productivity and dominance changes across environmental gradients. We conclude that, along environmental and competition gradients, the plasticity of plant form and function is required to maintain the coordination of multiple resource capture and, hence, to sustain productivity and dominance.

1. Introduction

The outcome of biotic interactions is a dynamic process which entails '*the explicit inclusion of organismal trade-offs, of environmental constraints, and of the basic mechanisms of interspecific interactions*' (Tilman, 1990) to be predictable. In a companion paper (Soussana et al., 2012), we present the Gemini model (Grassland Ecosystem Model with INdividual centred Interactions), which couples within a common modeling framework: carbon, nitrogen and water cycles (*ecosystem scale*), plant population dynamics based on resource competition (*community scale*) and physiological and morphological plasticity of clonal plants (*organismal trade-offs*).

An individual-centred approach was used to develop this coupling across scales and, hence, to develop a dynamical structure-function-diversity model capable of simulating the dynamics of plant species within a community as well as the role of traits and their plasticity for ecosystem functioning (Soussana et al., 2012; Maire, 2009). Gemini is an individual-centred model, rather than being individual-based, since it simulates average individuals within each plant population. Here we show that the details of physiological, morphological and demographic mechanisms allowing plant and population plasticity in the model are both necessary and sufficient (according to the parsimony principle) to simulate major trends in productivity and dominance across the perennial grass species studied.

The individual-based modeling approach offers the possibility to simulate the plastic adjustments of plant form and function in response to resource levels mediated by interactions with neighbors (Höglind et al., 2001; Yin and Schapendonk, 2004). Such plastic responses are shown to be mainly phenotypic (Grassein et al., 2010), species-specific and sometimes adaptive when they are correlated positively to changes in plant growth (Useche and Shipley, 2010a, 2010b; Pontes et al., 2010). Competition / facilitation biotic interactions are in part determined by these plastic responses of plants to resource levels (Grime, 1973; Tilman,

691984), which may enhance species coexistence and complementarity in plant communities 70(Soussana and Lafarge, 1998). For instance, Van Ruijven and Berendse (2003) have shown a 71reduction of leaf nitrogen content associated with higher plant nitrogen use efficiency when 72species grew at higher diversity level, enhancing the complementarity of nitrogen use and the 73functioning of grassland community. Therefore, mechanisms underpinning species plasticity 74are a prerequisite to explain species assembly rules in grassland communities and their 75consequences for ecosystem functioning (Grime and Mackey, 2002). Structure-function-76diversity models like GEMINI can help in understanding the role of plasticity for the adaptation 77of plant populations to environmental gradients across species diversity levels.

78 Phenotypic plasticity is only adaptive if it is properly co-ordinated with environmental 79fluctuation (Sultan, 2004; De Jong, 2005), *i.e.* when a plant modifies its phenotype by an 80appropriate amount and at a certain speed in order to optimize growth and fitness (Useche et 81al., 2010a). This principle is applied in the GEMINI model (see the companion paper, Soussana 82et al., 2012 for full details) through a coordination of above and below-ground resource 83capture that ensures that no resource is in excess (Chapin, 1991) and through the coordination 84of morphogenesis and of assimilate supply. First, physiological plasticity to light and nitrogen 85levels is obtained by combining: i) the functional balance hypothesis (Davidson, 1969; 86Wilson, 1988), which assumes that partitioning of growth between shoots and roots tends to 87balance shoot photosynthesis and root N acquisition to ensure C and N homeostasis; ii) the 88photosynthesis coordination hypothesis (Chen et al., 1993, Maire et al., 2012), which assumes 89that partitioning between shoot structures and photosynthetic proteins maintains a leaf protein 90content co-limiting the dark (Rubisco activity) and light driven (RuBP regeneration) reactions 91of C_3 leaf photosynthesis. Second, morphological plasticity is obtained by assuming a 92potential morphogenesis which adjusts the emission, the elongation and the senescence of 93leaves and roots in function of daily temperature and photoperiod and of daily temperature

and soil nitrogen concentration, respectively (Lemaire, 1999; Wu et al., 2004). Third, at the population scale, daily temperature and PAR (photosynthetically active radiation) fraction at the bottom of the canopy determine the plant axis ramification process (Neuteboom and Lantinga, 1989; Lafarge et al., 2005). Finally, plant growth is simulated as the minimum between supply (assimilate partitioning and reserves remobilization) and demand (morphogenesis and ramification) limited growth rates.

In this second paper, we focus on the role of physiological, morphological and population plasticity for species net primary productivity (an estimator of fitness for clonal plants) along resource (nitrogen), disturbance (cutting frequency) and competition (mixtures versus monocultures) gradients. We first evaluate the ability of the model to account for well-established empirical laws concerning: i) resource-based adjustments in root / shoot ratio, ii) self-thinning, iii) critical shoot N content, and iv) role of plant traits (specific leaf area and plant height) for responses to environmental gradients (nitrogen and disturbance). By comparing model versions of different complexity, we then test the following hypothesis: plant morphological (root and shoot morphology) and physiological (leaf N content, leaf photosynthesis) plasticity, as well as plant population (axis density) plasticity, are needed for maintaining population fitness (*i.e.* above-ground net primary productivity) across resource, disturbance and competition gradients.

2. Methods

2.1. Model purpose

The model is described following the ODD (Overview, Design concepts and Details) standard protocol proposed by Grimm et al. (2006) for individual-based and agent-based models in Soussana et al. (2012). A detailed list of all 132 equations, as well as the 187 variables and the

100 default parameter values and their units is available (at www1.clermont.inra.fr/urep/modeles/gemini.htm) and will be send on request.

The main purpose of GEMINI is to understand the dynamics and plasticity of plant species within a community and the role of traits and their plasticity for ecosystem functioning. The model considers climatic (short-wave radiation, temperature and precipitation) and atmospheric (CO_2 concentration) abiotic drivers. Management conditions concern both disturbance (through defoliation) and fertilization (inorganic and organic N supply). The model was built with a modular architecture, which allows the inclusion, or not, of a range of biotic agents (plant species, soil microbial decomposers and domestic herbivores) as well as environment and management modules (soil, vegetation, fertilization and cutting).

GEMINI can simulate a potentially unlimited number of plant species (or plant populations from the same species) from currently two plant functional types (perennial grasses and legumes). The model focuses on the acquisition and the utilization of two major resources (light and nitrogen) by plants and their consequences for the carbon and nitrogen cycles.

2.2. State variables and scales

GEMINI consists of vegetation, soil and herbivore sub-models, coupled with environment and management sub-models (for a full description of the model, see Soussana et al., 2012). The vegetation sub-model, named CANOPT is an individual-centred model of a multi-species stand comprising clonal grasses and/or legumes and forming a multi-layer plant canopy. Each clonal plant population is described as a collection of identical axes (*e.g.* tillers for grasses). Moreover, all plant species are assumed to be perfectly mixed in the horizontal plane. Plant population demography is calculated from the vegetative multiplication and mortality of axes. Other demographic processes, including flowering, fruiting, dispersion, germination and recruitment from seeds are not considered, since these processes are minimized by regular

disturbance through cutting and grazing in temperate grasslands dominated by perennial clonal pasture species (*e.g.* Harper, 1978).

The vegetation sub-model consists of four modules: i) a biochemical module, which simulates the C and N balance and the partitioning of growth among shoot structures (W_S), leaf proteins (W_P) and roots (W_R) for mean plant axes in each plant population. For each plant population, the corresponding state variables are the axes number (D, m^{-2}), and the mass per axis of three structural compartments (W_S, W_P and W_R) and of C and N substrates and of two C and two N reserve compartments; ii) a shoot morphogenesis module, which computes the demography and size of leaves (two state variables, length and mass per leaf); iii) a root morphogenesis module, which computes the demography and size of roots (two state variables, length and mass per root); iv) a competition module which calculates short-wave radiation and inorganic N partitioning among mixed plant populations.

The environment sub-model calculates the microclimate within the canopy and the inorganic N balance of the soil (or of the substrate when the vegetation model is not coupled to the soil model). The management sub-model schedules events caused by grassland management (cutting dates, grazing periods, N fertilizer applications).

2.3. Model parameterization and evaluation

The experimental site used for model calibration was established in spring 2002 in an upland area of central France (Theix, 45°43′N, 03°01′E, 870 m a.s.l.) on a granitic brown soil (Cambisol, FAO). The local climate is semi-continental, with a mean annual temperature of 9°C and a mean annual rainfall of 760 mm. 13 native perennial C_3 grass species that co-occur in mesic permanent grasslands were studied in monocultures: *Alopecurus pratensis*, *Anthoxanthum odoratum*, *Arrhenatherum elatius*, *Dactylis glomerata*, *Elytrigia repens*, *Festuca arundinacea*, *Festuca rubra*, *Holcus lanatus*, *Lolium perenne*, *Phleum pratense*, *Poa*

168*pratensis*, *Poa trivialis*, *Trisetum flavescens*. A *Lolium perenne* cultivar ('Clerpin') was added
169as a control. Henceforth, species are referred to by their species (*e.g. A. pratensis*) name.

170 The calibration procedure of the model has been reported by Soussana et al., (2012).
171Briefly, out of a total of 100 parameters, 65 have been considered as constant across the grass
172species investigated with a value taken from the literature. The remaining parameters were
173estimated by species from plant trait values measured in a non-limiting nutrient treatment
174(360 kgN ha^{-1} yr^{-1}; 3 cuts yr^{-1}) of the field experiment comparing 13 grass species grown in
175monocultures (see the calibration of these parameters in Soussana et al., 2012). In this
176treatment, neither nutrients nor water resources were limiting above-ground grass growth
177(Pontes et al., 2007, Maire et al., 2009).

178 Two parameters (LL_{plast}, the branching order dependency of potential root length and
179*Tr*, the thermal time interval between two successive root emission events) were optimized by
180maximizing axis biomass (W_G). This first optimization was done on C-N+ management
181treatment using constant axis density for each species. The two population demography
182parameters (*intcl*, the clonal integration and $Tsen_0$, the lifespan of an axis) were then
183optimized by fitting simulated to measured tiller density (*D*) per unit ground area. This second
184optimization was done after the root parameters optimization.

185 Predicted and measured annual dry-matter yields were highly correlated without bias
186across species, N supply and cutting frequency treatments in monocultures and in mixtures of
187six species (Soussana et al., 2012). The GEMINI model could therefore simulate without bias
188responses to nitrogen and disturbance gradients of net primary productivity and of plant
189community structure.

190

191

192

2.4. Experimental design for testing the model against empirical laws

We have tested model patterns against four types of well-established empirical laws: i) changes in root:shoot ratio following an abrupt change in resource availability, ii) self-thinning, iii) critical shoot N content decline during shoot growth, and iv) role of plant traits (specific leaf area and plant height) for population response to environmental gradients (nitrogen and disturbance). These patterns were studied with monocultures grown under constant environmental conditions (T_a = 14°C, *PPFD* = 700 µmol m^{-2} s^{-1}).

First, short-term responses of model compartments to disturbance (cutting) and to nutrients stress (N deprivation) were tested. Two partitioning functions *P* and *Q* control the partitioning of dry matter between shoot and root structures and between shoot structures and shoot proteins, respectively. *P* is calculated as the functional balance between shoot C and root N capture rates (Eq. 1, adapted from Hilbert and Reynolds, 1991; see supplementary materials SI1 and SI2 in Soussana et al. (2012) for full details). *Q* is calculated following the coordination hypothesis of leaf photosynthesis (Chen et al., 1993; Maire et al., 2009).

$$P = \left(\frac{f_C}{f_N} \; \frac{\sigma_{r\_act} \, W_R \, lwr . f_{active\_root}}{\sigma_C \; LA} \right)^{q_1} \qquad \text{(Eq. 1)}$$

$$Q = \left(f_{np} \, W_p \, D \Big/ \sum_{z=1}^{m} N_{pac_z} \; LAI_z \right)^{q_2} \qquad \text{(Eq. 2)}$$

Where f_C / f_N is the C:N plant ratio, σ_{r_act} is the root N uptake rate, W_R is the root dry mass, *lwr* is the root area to mass ratio, f_{active_root} is the proportion of active roots, σ_C is the net photosynthesis rate, *LA* is the plant axis leaf area, f_{np} is the N fraction in shoot proteins, W_p is the shoot proteins mass, *D* is the axis density per unit ground area, N_{pac_z} and LAI_z are the coordinated leaf photosynthetic content and the leaf area index in layer z, respectively. Power coefficients q_1 and q_2 vary the degree of control on partitioning for *P* and *Q* variables, respectively.

A critical N concentration curve is defined as being the minimum plant N concentration allowing maximum growth rate and is related to stand dry matter accumulation by a negative power function in a number of C_3 species, including perennial forage grasses (Lemaire et al., 2008). The ability of the model to simulate critical shoot N content decline during canopy regrowth was tested by simulating *D. glomerata* monocultures grown under close to non-limiting nitrogen conditions (corresponding to the C-N+ experimental treatment).

Third, the model's ability to simulate self-thinning (*i.e.* the negative power law relating the individual mass and the density of population units; *e.g.* Harper, 1978) was tested across species in monocultures and for two N fertilizer supplies (N-, N+) at low cutting frequency (three cuts per year).

Finally, the ability of the model to reproduce species specific responses to disturbance and to nitrogen was tested for a range of measured plant functional trait values (*SLA*, specific leaf area and plant height) by using simulated log response ratios (LNRR). Log response ratios are the logarithms of the ratios of species performances along an environmental gradient (Suding, et al., 2003), here at low *vs.* high cutting frequency (from 3 to 6 cuts yr^{-1}) and at low vs. high N supply (from 12 to 36 g N m^{-2} yr^{-1}). A positive LNRR value indicates a higher species performance at the higher end of the gradient (*i.e.* at high cutting frequency and at high N). Conversely, a negative value indicates a lower species performance at the lower end of the gradient.

2.5. Testing the role of plant and population plasticity

To test the role of plasticity for net primary productivity and its stability along resource and disturbance gradients (see Fig. 1 for the conceptual design of the modeling experiment), the full GEMINI model (FP) was compared with simplified versions offering reduced plasticity (from RP_1 to RP_4) and reduced coordination of growth (RP_5 and RP_6):

241- RP_1, full model but without axis demography resulting in constant axis density,

242- RP_2, same as RP_1 but without explicit root morphogenesis,

243- RP_3, same as RP_1 but without explicit shoot morphogenesis,

244- RP_4, same as RP_1 but without explicit root and shoot morphogenesis,

245- RP_5, same as RP_4 but with equal distribution of assimilates to leaf structure and leaf proteins,

246- RP_6, same as RP_4 but with equal distribution of assimilates to leaf structure and roots.

247 The corresponding modules (*i.e.* axis demography, root and shoot morphogenesis, 248assimilate partitioning) were inactivated either by setting parameter values to zero, or by 249replacing them by fixed parameter values (Table 1).

250 In order to suppress axis demography in RP_1, *intcl* and $Tsen_0$ parameters were set to zero 251in the ramification module. In RP_2, RP_3 and RP_4, morphogenesis modules were replaced by 252constant parameter values by species (Fig. 1). In RP_2 and RP_4, root morphogenesis was 253replaced by two species-specific parameters: a constant area to mass ratio of roots (*lwr*) and a 254constant root senescence rate ($TRoot_{Sen}$). In RP_3 and RP_4, shoot morphogenesis was replaced 255by a constant leaf area ratio (*LAR*, leaf area to plant mass ratio) and by a constant shoot 256senescence rate ($TShoot_{Sen}$). In addition, the shoot architecture module was replaced by a 257constant plant canopy density (leaf area per unit canopy volume, C_H) and by a constant leaf 258angle (*theta*) (Table 1). In RP_5 and RP_6, fixed and equal assimilate fractions to leaf structure 259and leaf proteins (RP_5) and to leaf structure and roots (RP_6) were obtained by setting the value 260of q_2 and q_1 parameter to zero in Eq. 2 and 1, respectively.

261 The optimization procedure used for the full plasticity version (FP) was then applied to 262each reduced plasticity model version. In the reduced plasticity version RP_1, the two root 263parameters LL_{plast} (branching order dependency of potential root length) and *Tr* (thermal time 264interval between two successive root emission events) were optimized as in FP version.

Values of these parameters were calculated for each species using the outputs of previous equilibrium simulations for the C-N+ treatment (Table 1B).

Reduced and full plasticity model versions were first compared for monocultures. Three grass species, which are representative of three plant N strategies (Maire et al., 2009), were used: *A. odoratum* (short and exploitative grass), *A. elatius* (tall and exploitative grass), and *F. arundinacea* (tall and conservative grass). Then, in order to test the role of plasticity for the outcome of plant-plant interactions, model versions with full and reduced plasticity were compared with binary mixtures. Finally, simulated species and model versions were compared along resource and disturbance gradients: (i) a light gradient with 100, 80 and 60 % of the daily short-wave radiation (*PPFD*) of the experimental site; (ii) a nitrogen gradient contrasting fertilization supply rates of 360, 120 and 60 kgN ha^{-1} yr^{-1}; (iii) a disturbance gradient with 8, 6, 3 and 1 cuts yr^{-1}.

Simulations were run for 10 years with the experimental site climate (years 2003-2004 in loop for which data were available, see Pontes et al., 2007) and management conditions. Spin-up runs and a restart procedure allowed initializing plant populations close to steady-state. Simulations were stopped for a given plant population whenever the substrate C mass tended towards zero (*i.e.* population death) or increased above an unrealistic value (greater than the plant structural C mass). Means were calculated over the simulation period of the plant population. With the FP model version simulations lasted in monocultures and mixtures 3655 and 3000 days, on average. With the RP_1 model version simulations lasted in monocultures and mixtures 2237 and 1715 days, on average. Within three species mixtures, the average duration of coexistence between two simulated species reached 473 days. Therefore, some of the simulations lasted for a shorter time period than 10 years.

2.6. Data analysis

An analysis of variance and Tukey's post-ANOVA comparisons at a p-level of 5% were used to analyze simulated above-ground net primary productivity (ANPP) across species, plasticity levels and environmental gradients in both monocultures and mixtures. Moreover, these tests were also applied to model outputs indicating light and nitrogen capture: the absorbed fraction of photosynthetically active radiation (*FAPAR*) and the nitrogen uptake rate per unit root area (*Su*). All statistical tests were performed with the software - Statgraphics Plus (Manugistics, Rockville, MD, USA).

3. Results

3.1. Simulating co-limitation of growth by light and inorganic N capture

After a cut, the *P* partitioning variable peaks at a high value thereby increasing partitioning to shoot structures at the expense of partitioning to root structures. During shoot regrowth after cutting, the gradual increase in photosynthesis leads to an exponential decline in *P* which tends asymptotically to one (Fig. 2A). This indicates the reestablishment of a functional balance between roots and shoots. Cutting also induces a sharp drop in the second partitioning variable (*Q*) as the residual leaf area becomes exposed to full radiation. This increases the leaf N content required for photosynthetic coordination, leading to an increased partitioning to leaf photosynthetic proteins at the expense of leaf structures. During shoot regrowth, photosynthetic proteins replenishment increases asymptotically *Q* value towards one and leaf photosynthesis coordination is re-established. Within one month after a cut, as *P* and *Q* values both converge towards one, growth is again co-limited by nitrogen, light and CO_2 capture.

In the same way, after nitrogen deprivation a reduced root inorganic N uptake leads to a decline in *P* value (Fig. 2B) and, thereby, to a preferential partitioning of assimilates to roots compared to shoot structures. Both increased root growth and a de-repression of root N uptake

315capacity (Soussana et al., 2012) lead to a restoration of N uptake and to an asymptotic
316increase of *P* value towards one. *Q* is little affected by inorganic N deprivation (Fig. 2B) and
317its value stays close to one. Hence, by adjusting their root:shoot ratio and their N uptake
318capacity, N deprived plants tend towards a co-limitation of growth by nitrogen uptake and by
319photosynthesis. P and Q values show oscillations over a few days (Fig. 2). Such oscillations
320are caused by the emission and senescence of individual leaves and roots, which alters
321root:shoot functional balance through small changes in leaf and root area.
322

323**3.2. Critical shoot nitrogen content decline**

324Critical shoot N content (see Methods) declines with above-ground biomass (Lemaire et al.,
3252008) according to a power law. This empirical law was tested with *Dactylis glomerata* under
326close to non-limiting nitrogen conditions (corresponding to the C-N+ experimental treatment).
327During the first part of the regrowth, simulated shoot N concentration fits to the empirical law
328(Fig. 3), showing that this law may therefore be a consequence of coordinated plant growth.
329However, above a leaf area index of 5 simulated changes in shoot N content slightly
330underestimate the empirically established critical nitrogen decline curve.
331

332**3.3. Simulating size vs. density relationships**

333Between species variations in mean individual shoot mass (W_S+W_P) and mean density (*D*) of
334plant axes were negatively correlated according to a power law (exponent -0.94, Fig. 4A).
335Data obtained in spring in the field experiment (Maire, 2009) showed a similar exponent (-
3361.12) between mean shoot tiller mass and tiller density (Fig. 4B). Simulations of size vs.
337density relationships with both shoots and roots (Fig. 4A, W_G) indicated a lower exponent in
338absolute value (close to -¾) of the size vs. density relationship. Therefore, the model captures
339an essential property of plant canopies that relates the size and density of a plant population.

3.4. Predicted productivity vs. traits relationships.

The simulated log-response ratio (LNRR) of above-ground net primary productivity (*ANPP*) to cutting frequency is significantly and positively correlated with *SLA* (r^2 = 0.59, p < 0.01, Fig. 5A). This indicates that the higher the *SLA* of the species, the higher its biomass at high compared to low cutting frequency. In the same way, the LNRR of *ANPP* to N supply is significantly and negatively correlated with plant height (r^2 = 0.36, p < 0.05, Fig. 5B). Hence, the lower the plant height, the higher its biomass at high compared to low N supply. Overall, these two results indicate that simulated species response to cutting frequency and N fertilization varies with plant functional traits and therefore with the functional strategy of species.

3.5. Plant plasticity and simulated above-ground productivity in monocultures

The role of plasticity for *ANPP* and its stability along cutting frequency, N supply and light gradients was tested with three grass species that are representative of contrasting N strategies (Maire et al., 2009) (Fig. 6, Table 2A). The full model (FP) provided a higher *ANPP* (Tukey's post-ANOVA comparison of multiple means, p < 0.05) than other model versions that restricted plasticity and coordination (Fig. 6). An intermediate *ANPP* was obtained for model versions without tiller dynamics and/or root, shoot morphogenesis (RP_1, RP_2, RP_3 and RP_4 versions). Model versions which, moreover, suppressed coordination between shoot structures and roots, or between shoot structures and leaf proteins (RP_5 and RP_6) had significantly lower *ANPP* (Tukey, p < 0.05) than other versions. The large role of plasticity for *ANPP* was underlined by a 51 % share of total variance for this factor and its interactions with others.

Radiation and nitrogen captures (*FAPAR* and S_u, respectively) also varied strongly with plasticity level (42 and 32 % of total variance, Table 2A). An explicit root morphogenesis (RP_1, RP_2 and RP_4) significantly increased root uptake activity (S_u) compared to model

versions without root morphogenesis and architecture (Tukey, $p < 0.05$, data not shown). An explicit shoot morphogenesis (FP, RP_1 and RP_2 versions) increased the absorbed radiation (*FAPAR*) compared to intermediate plasticity (RP_3 and RP_4) (data not shown).

With full plasticity (FP), the three grass species showed contrasting behaviors in response to environmental gradients. *ANPP* responses to N fertilization indicated a strong increase for all species, except *F. arundinacea* which reached a plateau (Fig. 6). *ANPP* responses to cutting frequency were smaller than with N supply and displayed contrasted slopes among species (see FP Fig. 6). *F. arundinacea* reached its optimum *ANPP* around 3 cuts per year; *A. elatius* around 6 cuts yr^{-1} and *A. odoratum* between 6 and 8 cuts yr^{-1} (Fig. 6). *F. arundinacea* *ANPP* decreased strongly with increasing shade, while the two other species were less affected (Fig. 6). In contrast to the full model version (FP), there was almost no increase in *ANPP* for the least plastic versions (RP_5 and RP_6) when light and N supply levels were increased and when disturbance level was reduced (Fig. 6).

3.6. Plasticity, productivity and dominance in binary mixtures

Within binary mixtures, the fraction of total variance (12, 24 and 33% for *ANPP*, *FAPAR* and S_u, respectively, Table 2B) attributed to the plasticity level was relatively smaller than in monocultures. However, the plasticity x species interaction explained also a substantial share of the total variance (17 and 39%, respectively) of *ANPP* and of *FAPAR*. The decline in *ANPP* at reduced plasticity levels was not systematically observed in mixtures. However, *ANPP* was always low when growth partitioning coordination was suppressed (RP_5, RP_6, Fig. 7).

In simulated binary mixtures, the dominance of *F. arundinacea* markedly declined with cutting frequency (Fig. 7). At three cuts per year, this tall grass overcompeted simulated *A. odoratum* and *A. elatius*, which were conversely dominant at higher cutting frequencies (Fig.

3907). This disturbance induced change in dominance became less marked when root and shoot
391morphogenesis were not modeled explicitly (RP_1 and RP_2) and was suppressed when growth
392partitioning coordination was knocked out (RP_5 and RP_6). In the latter case, the ANPP of
393simulated *F. arundinacea* was always close to zero (Fig. 7).

394 Within simulated mixtures of *A. odoratum* and *A. elatius*, *A. elatius* became increasingly
395dominant at high compared to low frequency when full plasticity was included. In contrast,
396when explicit root and shoot morphologies were suppressed (RP_2, RP_3 and RP_4), *A. odoratum*
397was favored by an increased cutting frequency (Fig. 7). Therefore, the outcome of simulated
398biotic interactions depended upon model assumptions on the degree of plant plasticity.

399

400**4. Discussion**

401By combining an individual-centred approach with coordination hypotheses, we have
402developed a mechanistic model linking plant functional traits, plant population and plant
403community dynamics and ecosystem processes (*e.g.* net primary productivity). In agreement
404with our initial hypothesis, we have shown through a modeling experiment that both
405individual plant plasticity and population plasticity are needed to maintain grass species
406fitness (i.e. above-ground net primary productivity) along gradients of resource levels
407(nitrogen, light), disturbance (cutting frequency) and competition (mixtures vs.
408monocultures). Moreover, emergent properties arising from the model with full plasticity
409account for four well-established empirical laws: i) resilience to defoliation and to N
410deprivation, ii) critical N decline during stand growth, iii) self-thinning and iv) trait mediated
411species productivity response to defoliation and N deprivation. Furthermore, simplified
412versions of the model lacking processes controlling plant plasticity and population plasticity
413display a lower net primary productivity as compared to the full plastic model.

414

4.1. Emergent properties of the model

At full complexity, the model presents emergent properties, which account for four well-established empirical laws.

First, the GEMINI model re-establishes a functional balance after a disturbance caused by defoliation and after a stress caused by N deprivation. After a defoliation event, a preferential partitioning of substrates first to leaf proteins and then to shoot structures is induced at the expense of roots. This response to defoliation replenishes leaf N content and increases leaf area. Conversely, after N deprivation, preferential partitioning to roots takes place and the activity of root transporters is de-repressed which also contributes to increased N uptake, thereby restoring a functional equilibrium and a coordination of leaf photosynthesis. Hence, through changes in the relative sizes and physiological activities of roots and shoots, plant growth will again be co-limited by multiple resources capture (photosynthetically active radiation, atmospheric CO_2 and inorganic N).

Second, the model accounts for the decline in critical N concentration during stand regrowth. Even when there is ample supply of N, plant shoot N concentration declines during growth within dense canopies. This observation led to the development of a law relating critical shoot N concentration (see Methods) and stand dry matter accumulation by a negative power function (Lemaire et al., 2008). For LAI values below ca. 5, this empirical law is well accounted for by the model. This shows that when leaves become gradually shaded, changes in leaf proteins to structure ratio support the hypothesis of leaf photosynthesis coordination (Maire, 2009). Through changes in the *Q* partitioning variable, an increasing fraction of shaded leaves induces the simulated decline in shoot N concentration during canopy growth. In contrast, simulated N content of leaves in full light at the top of the canopy remain constant (data not shown), in agreement with previous measurements (Gastal and Lemaire, 2002). At high *LAI* values (above 5), the empirical critical N content is slightly above the coordinated

simulated leaf N content. Overall, it is remarkable that the value and plasticity of C-N stoichiometry (see Gruber and Galloway, 2008) during autotrophy is an emergent property of coordinated resource acquisition by plants.

Third, self-thinning, a well-established empirical law is also predicted. The self-thinning rule relates plant mass to plant density in crowded, even-aged stands by a power-law equation with a negative exponent which is usually close in absolute value to 3/2. The rule is widely accepted as an empirical generalization and quantitative law that applies across the plant kingdom (*e.g.* Sackville-Hamilton et al., 1995; West et al., 1999). It is remarkable that the combination in the GEMINI model of detailed ecophysiological and morphogenetic processes at the individual plant scale results in a self-thinning rule relating size and density of tillers across grass species. Interestingly, both the model and the measurements show a negative exponent close to one, and therefore substantially lower than the 3/2 exponent (but see Enquist and Niklas, 2002). This could be caused by the physiological integration among tillers within clonal grasses which tends to reduce tiller mortality within crowded stands (De Kroon et al., 1992).

Finally, another emerging model property concerns its ability to explain some of the observed trait mediated species productivity responses to defoliation and N deprivation. The correlation between the log-response ratio of *ANPP* to cutting frequency and *SLA* is in good agreement with previous observations (Caldwell, 1981; Westoby, 1999) showing that high *SLA* favors fast leaf regrowth and hence a tolerance response to defoliation, by increasing the rate of leaf recovery (Gross et al., 2007). Similarly, the negative correlation between the log-response ratio of *ANPP* to N supply and plant height is consistent with the positive relationship which was found between plant height and N conservation with the same grass species (Maire et al., 2009).

4.2. Role of plasticity

The plasticity of traits can be influenced by allometric or physiological constraints and some species might be less plastic than others depending on their traits (Givnish, 2002; Enquist and Niklas, 2002; Weiner, 2004). However, to date, few studies have investigated relationships between trait plasticity and the variations of physiology, morphology and growth across plant species (Ackerly and Sultan, 2006).

The present modeling study supports the hypothesis that plasticity favors the resilience along nutrients and disturbance gradients of plant production and competitive ability (Figures 6, 7, 8) in agreement with previous reports (*e.g.* Soussana and Lafarge, 1998). With an individual centered-model such as GEMINI, suppressing axis demography (RP_1 version) halved the overall mean *ANPP* simulated by the model. Plastic adjustments in tiller density have been observed in response both to cutting frequency and to nitrogen supply (Lemaire and Chapman, 1996). Indeed, the negative exponent between tiller size and density shows that these two traits co-vary both within and across grass species. Imposing a constant tiller density, leads either to excess C and N substrates (under environmental conditions favorable for growth), or to substrate deficiency whenever resources become too limited to support the tiller population (data not shown).

Although suppressing shoot morphogenesis simulation (RP_2) did not affect significantly *ANPP*, suppressing both root morphogenesis and axis demography (RP_3) reduced by a factor of four *ANPP* in comparison to the full model. Therefore, root architecture and turnover appear to have a major role in an individual-centred model, since they contribute to the stability of yield along resource and disturbance gradients. Finally, further suppressing growth coordination (RP_5 and RP_6) leads to a mean *ANPP* that is divided by a factor of 1.25 or more compared to the full model, which underlines the major role of growth and photosynthesis coordination (Fig. 8).

These simulations reveal that although simple compartment-based models may be successful at predicting the instantaneous fluxes exchanged between vegetation and the environment, they are not applicable at the individual plant and population scales. Given the large variability in resource levels and in microclimate experienced by individual plants within stands, most assumptions of simple models (*e.g.* constant radiation and nitrogen use efficiencies) do not hold at this scale (Faurie et al., 1996; Gastal and Lemaire, 2002). In contrast, individual centered models show that plasticity in the form and function of individual plants stabilizes productivity, light interception and N uptake, as well as radiation and N use efficiencies (data not shown).

When applying the full model to binary mixtures, simulated grass species dominance was consistent with observations of:

- an increased dominance of grass species which have high plant stature and conservative traits (such as *F. arundinacea*) at low compared to high cutting frequencies, compared both to short and to tall exploitative grasses (*e.g. A. odoratum* and *A. elatius*), (Louault et al., 2005; Pontes et al., 2011);
- an increased dominance of tall vs. short exploitative grass species (*A. elatius vs. A. odoratum*) at low compared to high cutting frequencies (Grime, 1979; Pontes et al., 2011).

Without an explicit root and shoot morphogenesis, grass species dominance was not altered along a disturbance gradient. Under increased disturbance by cutting, species ability to rapidly emit new leaves is an important trait that favors competitive ability for light capture (Cingolani et al., 2005). Therefore, without explicit shoot morphogenesis, this capacity is lost and changes in dominance with cutting frequency are not simulated adequately anymore.

4.3. Model complexity

There is a common understanding that the complexity of a particular system is linked to the difficulty in predicting the system properties despite a detailed knowledge of the system elements and their relationships (Weaver, 1948; Heylighen, 2008). Complexity can be seen either as disorganized or as organized. The latter case applies to our study since we consider non-random and correlated interactions between a range of processes at the root, shoot, plant, population, community and ecosystem scales. We have retained the emergence concept since our simulated system shows plasticity properties which are not dictated by the elementary parameters which are used for modeling these processes. To understand such organized complexity with emergent properties computer simulation was necessary (Hill, 1996).

In this way, we changed the granularity of different submodels of GEMINI in order to test their pertinence for the plant fitness in a given environment. This has been partially integrated in the software architecture by activating / deactivating some submodels (*e.g.* leaf and root architectures) that are replaced by more simplistic behaviors. However this replacement is not fully automated in GEMINI, and it should be interesting for a mechanistic model like GEMINI to push away the degree of granularity at will. The difficulty of changing model granularity lies in the issue of coupling models. Coupling models requires a framework and a methodology of development (Davis, 2001) accounting for the exchange of data between models which should be considered itself as a model (Winiwarter, 2005) as well as for the ordering of variables during the integration process, because a dependency between variables implies an order of computation. This issue requires being able to analyze the formulas when coupling models to find the dependencies between variables and set up a new ordering in the integration process. As GEMINI is developed in C^{++} language, one can consider

designing an EDSL (Embedded Design Specific Language) based on metaprogramming and operators overloading (Fowler, 2010).

5. Conclusion

The Gemini model provides a consistent trait-based mechanistic framework for modeling the role of grass diversity and plasticity on community dynamics and ecosystem functioning. In this paper, we have shown from *in-silico* experiments the role of morphological (root and shoot morphology) and physiological (leaf N content, leaf photosynthesis) plasticity, as well as population (axis density) plasticity, for plant population fitness (*i.e.* net primary productivity) across resource, disturbance and competition gradients. Moreover, we have shown that model versions for which plasticity has been suppressed are not able to reproduce observed changes in net primary productivity across environment and competition gradients. Therefore, the details of physiological and morphological mechanisms allowing adaptive plasticity in the Gemini model are both necessary and sufficient (in agreement with the parsimony principle) to simulate major trends in perennial grasses productivity and dominance. This modeling experiment shows that along environmental and competition gradients the plasticity of plant form and function contributes to maintain the coordination of multiple resource capture and, hence, to sustain productivity and dominance.

6. Acknowledgements

This study was financially supported by the French ANR DISCOVER (ANR-05-BDIV-010-01) and ANR QDIV (ANR-05-BDIV-009-01) projects and by the FEDER, 'l'Europe s'engage en région Auvergne'. V. Maire was funded by a Ph-D grant of French research ministry. We thank Hoglah Dasari and two anonymous referees which provide helpful comments and improvements on previous versions of the manuscript.

7. References

Ackerly, D., Sultan, S., 2006. Mind the gap: the emerging synthesis of plant 'eco-devo'. New Phytol. 170, 648-653.

Caldwell, M.M., 1981. Plant response to solar ultraviolet radiation. Pages 170-194 *in* L. e. A. éd., editor. Physiological plant ecology I. Springer Verlag, Berlin.

Chapin III, F.S., 1991. Integrated responses of plants to stress. A centralized system of physiological responses. Bioscience 41, 29-36.

Chen, J.L., Reynolds, J.F., Harley, P.C., Tenhunen, J.D., 1993. Coordination theory of leaf nitrogen distribution in a canopy. Oecologia 93, 63-69.

Cingolani, A.M., Posse, G., Collantes, M.B., 2005. Plant functional traits, herbivore selectivity and response to sheep grazing in Patagonian steppe grasslands. J. App. Ecol. 42, 50–59.

Davidson, R.L., 1969. Effect of root/leaf temperature differentials on root/shoot ratios in some pasture grasses and clover. Ann. Bot. 33, 561-569.

Davis, P.K., 2001. Adaptive designs for multiresolution multiperspective modeling (MRMPM). Pages 27-52 *in* Discrete event modeling and simulation technologies, Springer-Verlag.

De Jong, G., 2005. Evolution of phenotypic plasticity: patterns of plasticity and the emergence of ecotypes. New Phytol. 166, 101-117.

De Kroon, H., Hara, T., Kwant, R., 1992. Size hierarchies of shoots and clones in clonal herb monocultures: do clonal and non-clonal plants compete differently? Oikos 63, 410-419.

Enquist, B.J., Niklas, K.J., 2002. Global allocation rules for patterns of biomass partitioning in seed plants. Science 295, 1517-1520.

Faurie, O., Soussana, J.-F., Sinoquet, H., 1996. Radiation interception, partitioning and use in grass-clover mixtures. Ann. Bot. 77, 35-45.

588Fowler, M., 2010. Domain-specific languages. Addison—Wesley.

589Gastal, F., Lemaire, G., 2002. N uptake and distribution in crops: an agronomical and
590 ecophysiological perspective. J. Exp. Bot. 53, 789-799.

591Givnish, T.J., 2002. Ecological constraints on the evolution of plasticity in plants. Evol. Ecol.
592 16(3), 213-242.

593Grassein, F., Till-Bottraud, I., Lavorel, S., 2010. Plant resource-use strategies: the importance
594 of phenotypic plasticity in response to a productivity gradient for two sub-alpine species.
595 Ann. Bot. 106, 637-645.

596Grime, J.P., 1973. Competitive exclusion in herbaceous vegetation. Nature 242, 344-347.

597Grime, J.P., 1979. Plant strategies and vegetation processes. Wiley, J. & Sons Press,
598 Chichester, UK, 222 pp.

599Grime, J.P., Mackey, J.M.L., 2002. The role of plasticity in resource capture by plants. Evol.
600 Ecol. 16, 299-307.

601Gross, N., Suding, K.N., Lavorel, S. 2007. Leaf dry matter content and lateral spread predict
602 response to land use change for six subalpine grassland species. J. Veget. Sci. 18, 289-
603 300.

604Gross, N., Kunstler, G., Liancourt, P., Bello, F., Suding, K.N., Lavorel, S., 2009. Linking
605 individual response to biotic interactions with community structure: a trait-based
606 framework. Funct. Ecol. 23, 1167-1178.

607Gruber, N., Galloway, J.N., 2008. An Earth-system perspective of the global nitrogen cycle.
608 Nature 451, 293-296.

609Harper, J.L., 1978. Plant relations in pastures. In: Plant relations in pastures. Csiro (eds),
610 Melbourne, Australia, p. 1-14.

611Heylighen, F., 2008. Complexity and self-organization, in: Bates, M.J., Maack, M.N. (eds.),
612 Encyclopedia of Library and Information Sciences. CRC Press, Los Angeles, USA.

613Hilbert, D. W., Reynolds, J. F., 1991. A model allocating growth among leaf proteins, shoot
614 structure, and root biomass to produce balanced activity. Ann. Bot. 68, 417-425.
615Hill, D.R.C., 1996. Object-oriented analysis and simulation modeling. Addison Wesley
616 Longman, Boston, USA 291 pp.
617Hoglind, M., Schapendonk, A.. Van Oijen, M. 2001. Timothy growth in Scandinavia:
618 combining quantitative information and simulation modelling. New Phytol. 151, 355-367.
619Lafarge, M., Mazel, C., Hill, D.R.C., 2005. A modelling of the tillering capable of
620 reproducing the fine-scale horizontal heterogeneity of a pure grass sward and its
621 dynamics. Ecol. Model. 183, 125-141.
622Lemaire, G., Chapman, D., 1996. Tissue flows in grazed plant communities. In: Hodgson, J.,
623 Illius, A.W., (eds), The Ecology and Management of Grazing Systems, Wallingford, UK,
624 p. 3–36.
625Lemaire, G., 1999. Les flux de tissus foliaires au sein des peuplements prairiaux. Eléments
626 pour une conduite raisonnée du pâturage. Fourrages 159, 203-222.
627Lemaire G., Jeuffroy, M.H., Gastal, F., 2008. Diagnosis tool for plant and crop N status in
628 vegetative stage theory and practices for crop N management. Eur. J. Agron. 28, 614-624.
629Louault, F., Pillar, V.D., Aufrere, J., Garnier, E., Soussana, J.-F., 2005. Plant traits and
630 functional types in response to reduced disturbance in a semi-natural grassland. J. Veget.
631 Sci. 16, 151-160.
632Maire, V., Martre, P., Kattge, J., Gastal, F. Esser, G. Fontaine, S., Soussana, J.-F. The coordination of
633 leaf photosynthesis links C and N fluxes in C_3 plant species. Accepted in PlosOne.
634Maire, V., Gross, N., Pontes, L., Picon-Cochard, C., Soussana, J.-F., 2009. Trade-off between
635 root nitrogen acquisition and shoot nitrogen utilization across 13 co-occurring pasture
636 grass species. Funct. Ecol. 23, 668 - 679.

637Maire, V., 2009. From functional traits of grasses to the functioning of grassland ecosystem: a
638 mechanistic modelling approach. PhD thesis, Blaise Pascal University, Clermont-Ferrand,
639 France, 300 pp.
640Neuteboom, J.H., Lantinga, E.A., 1989. Tillering potential and relationship between leaf and
641 tiller production in perennial Ryegrass. Ann. Bot. 63, 265-270.
642Pontes, L.D.S., Soussana, J.-F., Louault, F., Andueza, D., Carrere, P., 2007. Leaf traits affect
643 the above-ground productivity and quality of pasture grasses. Funct. Ecol. 21, 844-853.
644Pontes, L.D., Louault, F., Carrere, P., Maire, V., Andueza, D., Soussana, J.F. 2010. The role
645 of plant traits and their plasticity in the response of pasture grasses to nutrients and cutting
646 frequency. Ann. Bot. 105, 957-965.
647Pontes, L.D., Maire, V., Louault, F., Soussana, J.F., Carrere, P., 2011. Impacts of species
648 interactions on grass community productivity under contrasting management regimes.
649 Oecologia in press.
650Sackville-Hamilton, N.R., Matthew, C., Lemaire, G., 1995. In defence of the -3/2 boundary
651 rule: a re-evaluation of self-thinning concepts and status. Ann. Bot. 76, 569-577.
652Soussana, J.-F., Lafarge, M., 1998. Competition for resources between neighbouring species
653 and patch scale vegetation dynamics in temperate grasslands. Ann. Zootechn. 47, 371-
654 382.
655Soussana, J.F., Maire, V., Gross, N., Hill, D., Bachelet, B., Pages, L., Martin, R., Wirth, C.,
656 2012. GEMINI: a grassland model simulating the role of plant traits for community
657 dynamics and ecosystem functioning. Part I: Parameterization and Evaluation. Ecol.
658 Model.
659Suding, K.N., Goldberg, D.E., Hartman, K.M., 2003. Relationships among species traits:
660 Separating levels of response and identifying linkages to abundance. Ecology 84, 1-16.

661Sultan, S.E., 2004. Promising directions in plant phenotypic plasticity. Perspect. Plant Ecol. 6,
662 227-233.
663Tilman, D., 1984. Plant dominance along an experimental nutrient gradient. Ecology 65,
664 1445-1453.
665Tilman, D., 1990. Constraints and tradeoffs: toward a predictive theory of competition and
666 succession. Oikos 58(1): 3-15.
667Useche, A., Shipley, B., 2010a. Interspecific correlates of plasticity in relative growth rate
668 following a decrease in nitrogen availability. Ann. Bot. 105, 333-339.
669Useche, A., Shipley, B., 2010b. Plasticity in relative growth rate after a reduction in nitrogen
670 availability is related to root morphological and physiological responses. Ann. Bot. 106,
671 617-625.
672Van Ruijven, J., Berendse, F., 2003. Positive effects of plant species diversity on productivity
673 in the absence of legumes. Ecol. Lett. 6, 170–175.
674Weaver, W., 1948. Science and complexity. American Scientist 36, 536-544.
675Weiner, J., 2004. Allocation, plasticity and allometry in plants. Perspectives Plant Ecol. Evol.
676 System. 6, 207-215.
677West, G.B., Brown, J.H., Enquist, B.J., 1999. A general model for the structure and allometry
678 of plant vascular systems. Nature 400, 664-667.
679Westoby, M., 1999. The LHS strategy scheme in relation to grazing and fire. In: People and
680 rangelands: building the future. International Rangeland Congress, Inc, Aitkenvale
681 Australia, Proceedings of the VI International Rangeland Congress, Townsville,
682 Queensland, Australia, Volumes 1 and 2, p. 893-896
683Wilson, J.B., 1988. A review of evidence on the control of shoot : root ratio, in relation to
684 models. Ann. Bot. 61, 433-449.

685Winiwarter, W., 2005. The interface problem in model coupling: examples from atmospheric
686 science. In Proceedings of the OICMS 2005 Conference, p. 43-48.
687Wu, Z., Skjelvag, A.O., Baadshaug, O.H., 2004. Quantification of photoperiodic effects on
688 growth of *Phleum pratense*. Ann. Bot. 94, 535-543.
689Yin, X., Schapendonk, A., 2004. Simulating the partitioning of biomass and nitrogen between
690 roots and shoot in crop and grass plants. Njas-Wageningen J. Life Sci. 51, 407-426.

TABLE CAPTIONS

Table 1. Parameter calibration of GEMINI for reduced plasticity versions (RP_{1-6}). The parameterization of the full plasticity version (FP) is reported by Soussana et al. (2012). A) Modeling experiment evaluating the role of plant plasticity. The full GEMINI model (FP) was compared with reduced demographic and morphogenetic plasticity (from RP_1 to RP_4) and with reduced coordination of growth (RP_5 and RP_6) versions. D_{Sp}, indicates that a dynamic variable is calculated by the model. P_{Sp}, indicates that a parameter has been calibrated for each species using pseudo-equilibrium FP output variables for the C- N+ experimental treatment (see Methods). B) Species-specific parameter values (P_{Sp}) in reduced plasticity versions. Abbreviations: *intcl*, clonal integration; $Tsen_0$, axis lifespan; q_1 and q_2, power coefficients varying the degree of control on partitioning between shoot and root structures and between shoot structures and leaf proteins, respectively; C_H, leaf canopy density; *LAR*, leaf area ratio; *theta*, leaf angle; $TShoot_{Sen}$, shoot senescence rate; $TRoot_{Sen}$, root senescence rate; *lwr*, root area ratio. nd; not determined.

Table 2. ANOVA (General Linear model) for the effects of plant species (*A. odoratum*, *A. elatius* and *F. arundinacea*), plant plasticity (FP, RP_1 to RP_6 versions of the model, see Methods), cutting frequency, incident light and nitrogen supply factors on simulated above-ground net primary productivity (*ANPP*), fraction of absorbed photosynthetically active radiation (*FAPAR*) and nitrogen uptake rate (*Su*). A) Monocultures, B) Binary mixtures. Abbreviations: df, degree of freedom; Expl. Var., percentage of variance explained; ns, not significant.

Figure Captions

Figure 1. Conceptual design of a modeling experiment for evaluating the role of plant plasticity. Aboveground net primary productivity (ANPP) is compared between full model (FP), reduced demographic and morphogenetic plasticity model versions (RP_1 to RP_4) and reduced coordination of growth (RP_5 and RP_6) model versions.

Figure 2. Effects of a cut (at 5 cm height on day 0) and of N deprivation (from 0.25 to 0.05 gN m^{-2} d^{-1} on day 110) on the *P* and *Q* variables partitioning assimilates between shoot and root structures, and between shoot structures and leaf photosynthetic proteins, respectively. Simulations were run with *D. glomerata* under a constant environment. Note that small oscillations in *P* and *Q* dynamics after disturbance by cutting and N deprivation are caused by changes in leaf and in root numbers (emission and mortality).

Figure 3. Simulated and empirical relationships between shoot N concentration and shoot dry matter during regrowth after a cut (open circles) for the C-N+ treatment. Open circles show simulation results. The solid line shows the empirical law relating critical shoot N concentration (Y, %) and shoot dry-matter (X, t DM ha^{-1}) as $Y = 4.8\ X^{-0.32}$ (Lemaire et al., 2008). The dashed line shows the fit of a power law to simulated results for shoot dry-matter values above 2.5 t DM ha^{-1}.

Figure 4. Relationships between simulated mean tiller mass (W_G), simulated shoot mass (W_S + W_P) and simulated mean tiller density (A); and between observed shoot mass and observed mean tiller density (B) across 13 grass species. Species abbreviations are: *Alopecurus pratensis* (*Ap*), *Anthoxanthum odoratum* (*Ao*), *Arrhenatherum elatius* (*Ae*), *Dactylis*

739*glomerata* (*Dg*), *Elytrigia repens* (*Er*), *Festuca arundinacea* (*Fa*), *Festuca rubra* (*Fr*), *Holcus*
740*lanatus* (*Hl*), *Lolium perenne* (*Lp*), *Lolium perenne* cultivar (Cl), *Phleum pratense* (*Php*), *Poa*
741*pratensis* (*Pp*), *Poa trivialis* (*Pt*), *Trisetum flavescens* (*Tf*). In A, simulated relationships for
742mean tiller mass (W_G) and for shoot mass ($W_S + W_P$) are displayed in capitals and in small
743letters, respectively. Simulations were run for 10 years in monocultures at 3 cuts per year and
744for 360 kgN ha^{-1} yr^{-1} N fertilizer supply. Slope and intercepts of SMA regressions were
745calculated according to Warton *et al.* (2006). In B, the observations of tiller density and shoot
746mass of grass species were measured under equivalent management in the site of Theix and
747were fully commented in Pontes et al. (2007) and in Soussana et al. (2012).
748
749**Figure 5.** Relationships between plant functional traits and above-ground net primary
750productivity (ANPP) response (log response ratio, LNRR, Suding et al. 2003) to management
751changes of 12 grass species simulated by GEMINI in monoculture. (A) Relationship between
752specific leaf area (*SLA*) and response to cutting intensity increase (LNRR(cut), from 3 to 6 cut
753yr^{-1}); (B) Relationship between plant height and response to N fertilization increase
754(LNRR(N), from 120 to 360 kgN ha^{-1} yr^{-1}).
755
756**Figure 6.** Simulated above-ground net primary productivity (ANPP) of three grass
757monocultures (*A. odoratum*, *A. elatius*, *F. arundinacea*) along disturbance (cutting frequency:
7581, 3, 6 and 8 cuts yr^{-1}), nitrogen supply (60, 120 and 360 kgN ha^{-1} yr^{-1} from substrate and
759fertilizer) and light (100, 80 and 60% of incident daily *PPFD*) gradients. The full GEMINI
760model (FP) was compared with versions increasingly (from RP_1 to RP_6) restricting plasticity
761and coordination of plant form and function (see Methods). RP_1, no axis turnover; RP_2, same
762as RP_1 but without explicit root morphogenesis; RP_3, same as RP_1 but without explicit shoot
763morphogenesis; RP_4, same as RP_1 but without explicit root and shoot morphogenesis; RP_5,
764same as RP_4 with equal distribution of assimilates to leaf structure and leaf proteins; RP_6,

same as RP_4 with equal distribution of assimilates to leaf structure and roots. The effects of plasticity level (P), of environmental gradients (C: cutting frequency, N: nitrogen fertilization level, L: light level) and of their interactions were tested by ANOVA (see SI3 for details) and are shown with their corresponding *p*-level.

Figure 7. Simulated above-ground net primary productivity (ANPP) of binary mixtures of *A. odoratum*, *A. elatius* and *F. arundinacea* along a cutting frequency (3, 6 and 8 cuts per year) gradient. Figures in the same row compare the two component species within a binary mixture. The full GEMINI model (FP) was compared with versions increasingly (from RP_1 to RP_6) restricting plasticity and coordination of plant form and function. For abbreviations, see Figure 8.

Figure 8. Simulated plasticity levels ratios for mean above-ground net primary productivity (ANPP) of grass species (*A. odoratum*, *A. elatius* and *F. arundinacea*) in monocultures and in binary mixtures across all N fertilization, cutting regime and light gradients. The plasticity level ratio was calculated as the ratio of a given plasticity level (FP, RP_1 to RP_5) to the lowest plasticity level (RP_6).

782**Table 1.**

A) Parameter of FP model	FP value	RP_1 value	RP_2 value	RP_3 value	RP_4 value	RP_5 value	RP_6 value
intcl	P_{Sp}	0	0	0	0	0	0
T_{sen0}	P_{Sp}	0	0	0	0	0	0
q_1	3	3	3	3	3	3	0
q_2	3	3	3	3	3	0	3
Output of FP model	FP value	RP_1 value	RP_2 value	RP_3 value	RP_4 value	RP_5 value	RP_6 value
$C_H = LAI / H$	D_{Sp}	D_{Sp}	D_{Sp}	P_{Sp}	P_{Sp}	P_{Sp}	P_{Sp}
$LAR = LAI / (D \cdot (W_S + W_P))$	D_{Sp}	D_{Sp}	D_{Sp}	P_{Sp}	P_{Sp}	P_{Sp}	P_{Sp}
$theta = {}_{layer}theta / i\ layers$	D_{Sp}	D_{Sp}	D_{Sp}	P_{Sp}	P_{Sp}	P_{Sp}	P_{Sp}
$TShoot_{Sen} = SA_{sen} / SA$	D_{Sp}	D_{Sp}	D_{Sp}	P_{Sp}	P_{Sp}	P_{Sp}	P_{Sp}
$TRoot_{Sen} = RA_{sen} / RA$	D_{Sp}	D_{Sp}	P_{Sp}	D_{Sp}	P_{Sp}	P_{Sp}	P_{Sp}
$lwr = RA / RM$	D_{Sp}	D_{Sp}	P_{Sp}	D_{Sp}	P_{Sp}	P_{Sp}	P_{Sp}

783

B) Species value (P_{Sp})	C_H $m^2\ m^{-3}$ leaf	***LAR*** $m^2\ g^{-1}$ leaf	***theta*** °	$TShoot_{Sen}$ d^{-1}	$TRoot_{Sen}$ d^{-1}	***lwr*** $m^2\ g^{-1}$ root
Alopecurus pratensis	14.58	0.0188	66.8	0.0253	0.0021	0.0557
Anthoxanthum odoratum	20.58	0.0208	59.7	0.0178	0.0179	0.1523
Arrhenartherum elatius	17.95	0.0233	65.0	0.0222	0.0107	0.0614
Dactylis glomerata	23.59	0.0185	70.1	0.0245	0.0087	0.0700
Elymus repens	18.20	0.0195	57.8	0.0240	0.0040	0.0616
Festuca arundinacea	22.77	0.0154	65.0	0.0111	0.0090	0.0914
Festuca rubra	28.64	0.0098	50.4	0.0164	0.0073	0.0865
Holcus lanatus	33.11	0.0246	70.1	0.0185	0.0158	0.1152
Lolium perenne	18.21	0.0179	70.5	0.0195	0.0008	0.0722
L. perenne var. Clerpin	18.99	0.0197	66.3	0.0167	0.0107	0.0625
Phleum pratense	26.36	0.0219	59.4	0.0185	0.0166	0.0944
Poa pratensis	32.76	0.0178	58.2	0.0135	0.0106	0.0903
Poa trivialis	nd	nd	nd	nd	nd	nd
Trisetum flavescens	17.54	0.0194	53.3	0.0250	0.0219	0.1257

784

785**Table 2**

A) Monoculture		***DMY***		***FAPAR***		***Su***	
Factors	**df**	**Expl. Var.**	***P***	**Expl. Var.**	***P***	**Expl. Var.**	***P***
Species	2	5.25	< 0.001	2.7	< 0.001	24.0	< 0.001
Plasticity	6	24.03	< 0.001	42.2	< 0.001	32.3	< 0.001
C	2	10.03	< 0.01	6.3	< 0.001	0.7	< 0.01
N	2	21.91	< 0.001	11.8	< 0.001	27.8	< 0.001
Light	2	0.47	< 0.01	3.7	< 0.001	3.0	< 0.001
Species*Plasticity	12	14.24	< 0.001	16.6	< 0.001	5.0	< 0.001
Species*C	6	0.74	< 0.01	-	ns	-	ns
Species*N	4	0.59	< 0.01	-	ns	-	ns
Species*Light	4	0.79	< 0.01	2.7	< 0.001	-	ns
Plasticity*C	18	11.48	< 0.001	-	ns	0.6	< 0.01
Plasticity*N	12	6.58	< 0.001	3.3	< 0.001	2.2	< 0.001
Plasticity*Light	12	2.57	< 0.001	7.5	< 0.001	4.3	< 0.001
C*N	6	1.32	< 0.001	1.0	< 0.01	-	ns
C*Light	6	-	ns	-	ns	-	ns
N*Light	4	-	ns	2.1	< 0.001	-	ns
Total	652	r^2 = 75.0	< 0.001	r^2 = 67.2	< 0.001	r^2 = 88.1	< 0.001

B) Mixture		***DMY***		***FAPAR***		***Su***	
Factors	**df**	**Expl. Var.**	***P***	**Expl. Var.**	***P***	**Expl. Var.**	***P***
Mixture	2	1.7	< 0.001	0.5	< 0.01	1.3	< 0.001
Species	2	0.9	< 0.001	-	ns	30.2	< 0.001
Plasticity	6	28.9	< 0.001	24.4	< 0.001	33.2	< 0.001
C	2	9.3	< 0.001	2.5	< 0.001	1.0	< 0.001
N	2	9.8	< 0.001	2.7	< 0.001	21.3	< 0.001
Light	2	0.9	< 0.001	-	ns	3.0	< 0.001
Mixture*Plasticity	12	3.9	< 0.001	8.6	< 0.001	1.7	< 0.001
Mixture*C	6	0.7	< 0.001	2.5	< 0.001	0.2	< 0.01
Mixture*N	4	0.6	< 0.001	-	ns	0.2	< 0.001
Mixture*Light	4	-	ns	-	ns	-	ns
Species*Plasticity	12	20.6	< 0.001	39.2	< 0.001	2.7	< 0.001
Species*C	6	4.5	< 0.001	12.3	< 0.001	1.0	< 0.001
Species*N	4	1.9	< 0.001	3.3	< 0.001	0.8	< 0.001
Species*Light	4	-	ns	-	ns	0.1	< 0.05
Plasticity*C	18	7.6	< 0.001	1.6	< 0.05	1.8	< 0.001
Plasticity*N	12	4.8	< 0.001	1.7	< 0.001	0.7	< 0.001
Plasticity*Light	12	2.6	< 0.001	-	ns	0.8	< 0.001
C*N	6	1.0	< 0.001	-	ns	0.2	< 0.01
C*Light	6	0.4	< 0.05	-	ns	-	ns
N*Light	4	-	ns	-	ns	-	ns
Total	1139	r^2 = 67.9	< 0.001	r^2 = 54.6	< 0.001	r^2 = 89.1	< 0.001

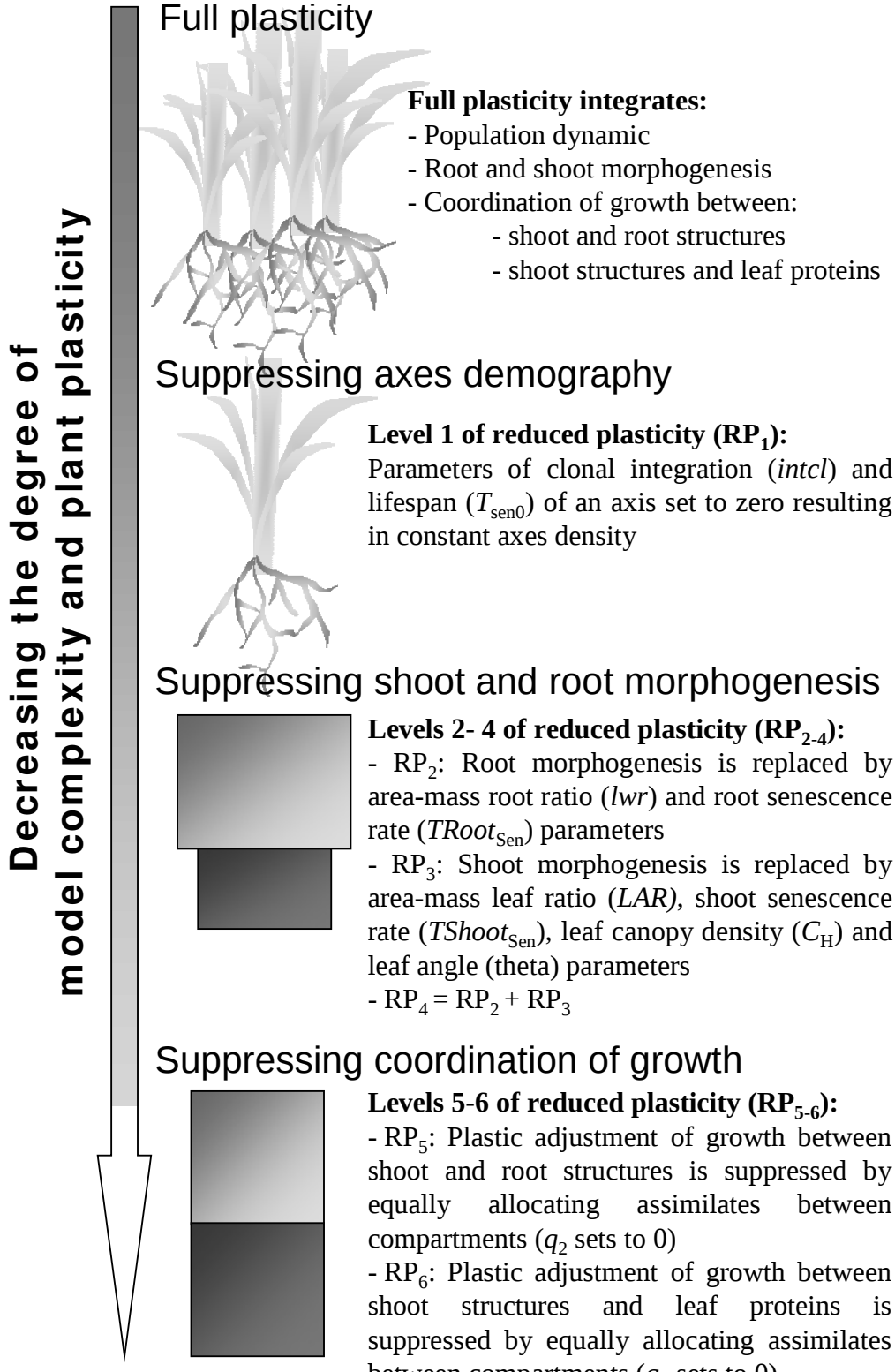

786

787**Figure 1**

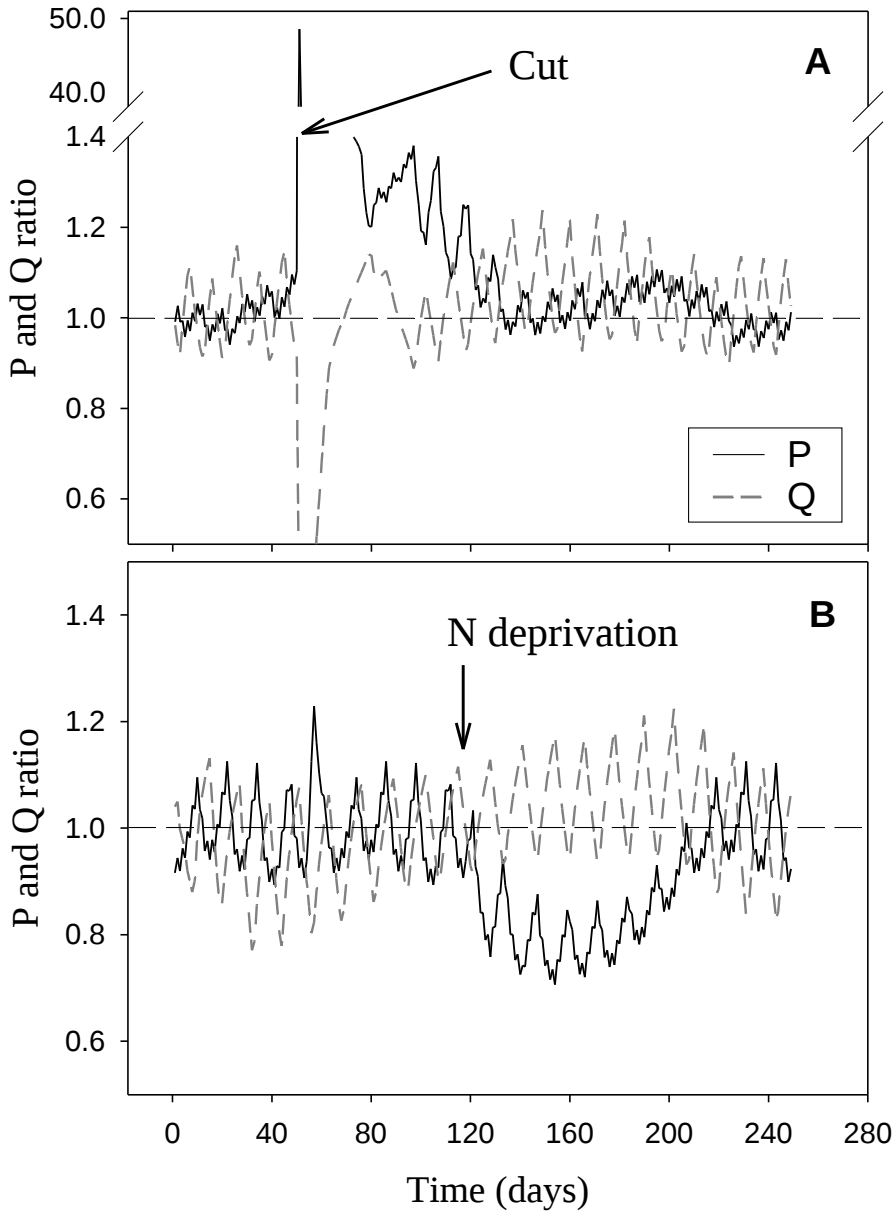

788

789**Figure 2**

37

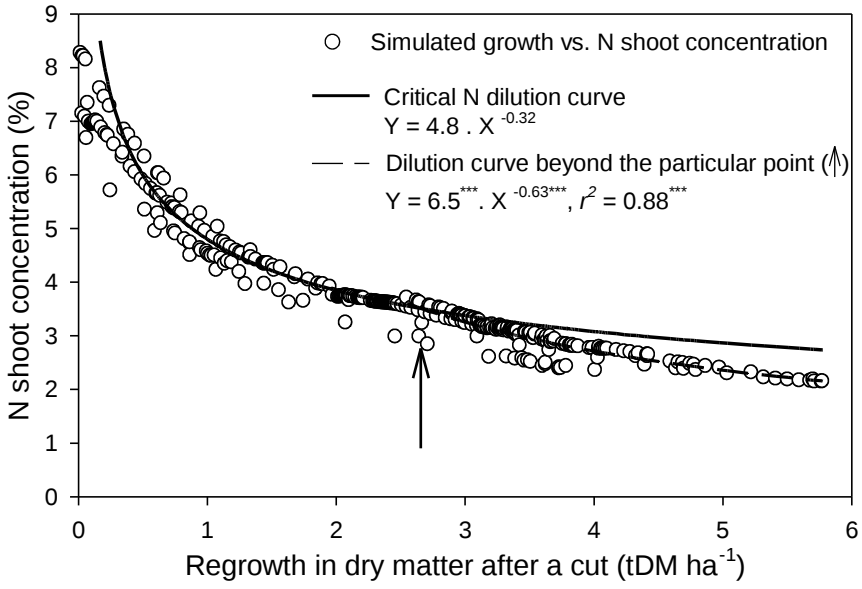

790

791**Figure 3**

38

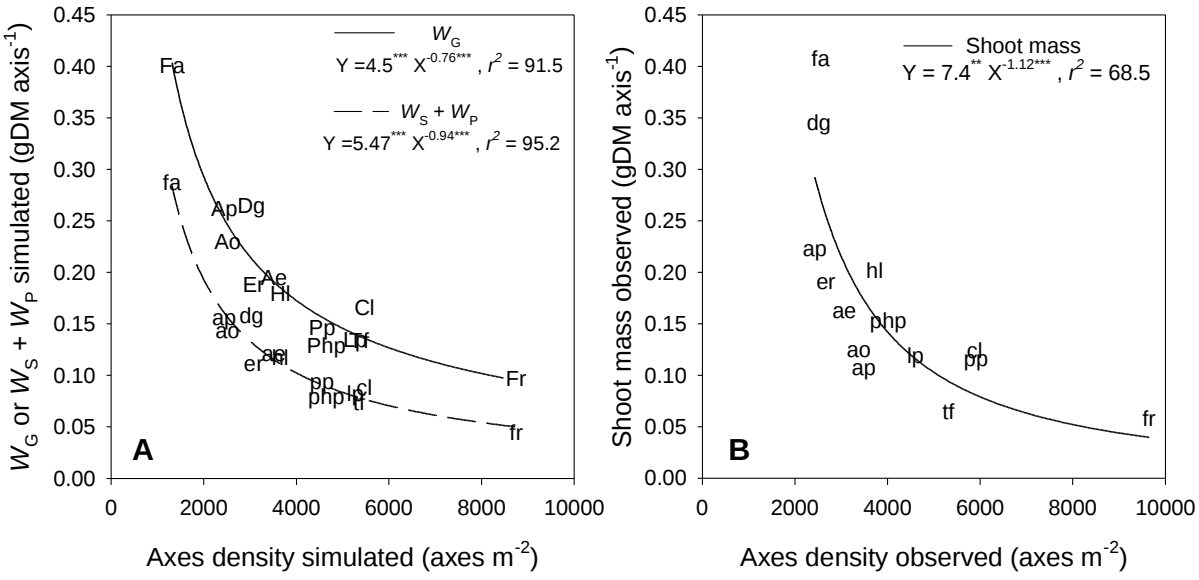

792

793**Figure 4**

39

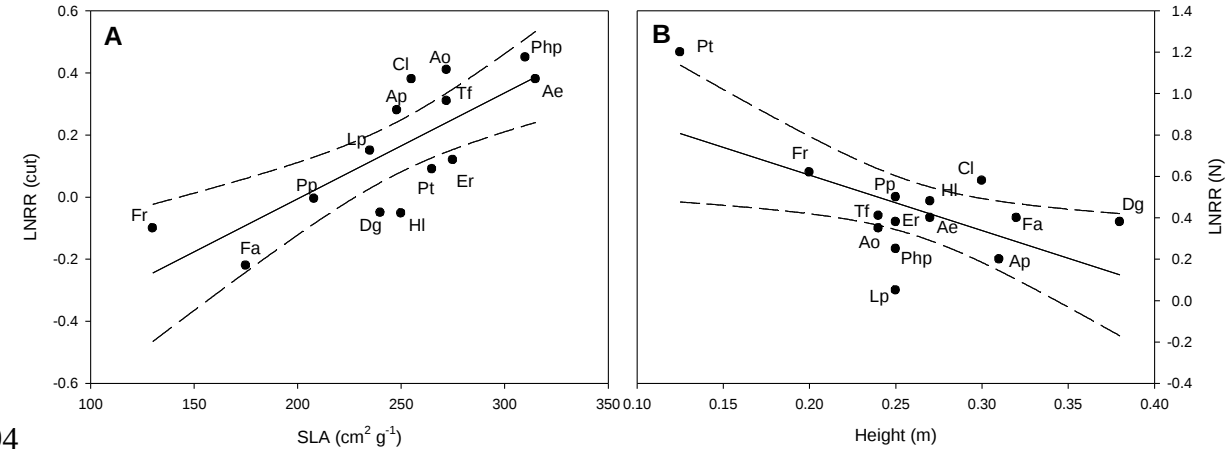

794

795**Figure 5**

40

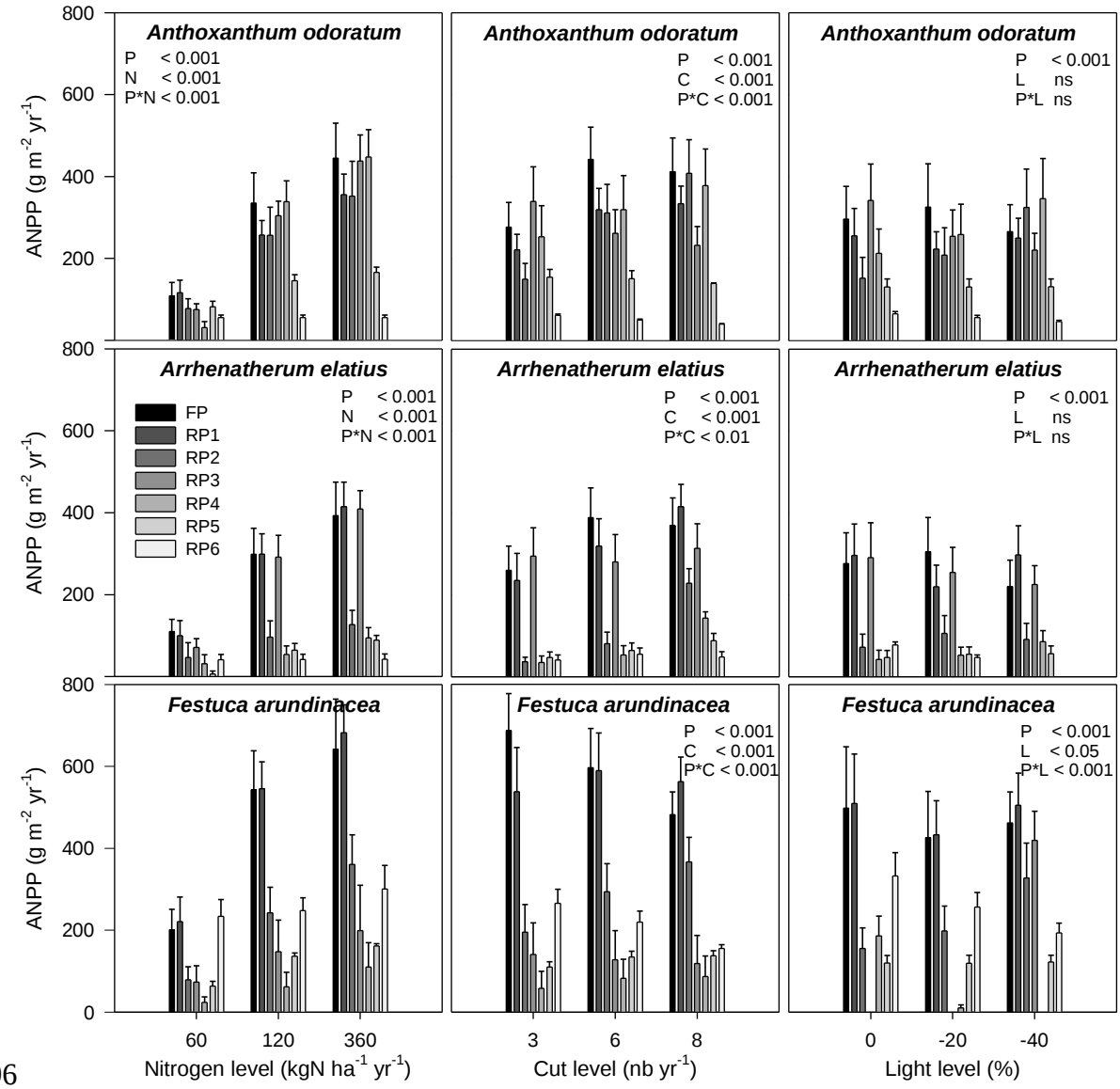

796

797**Figure 6**

41

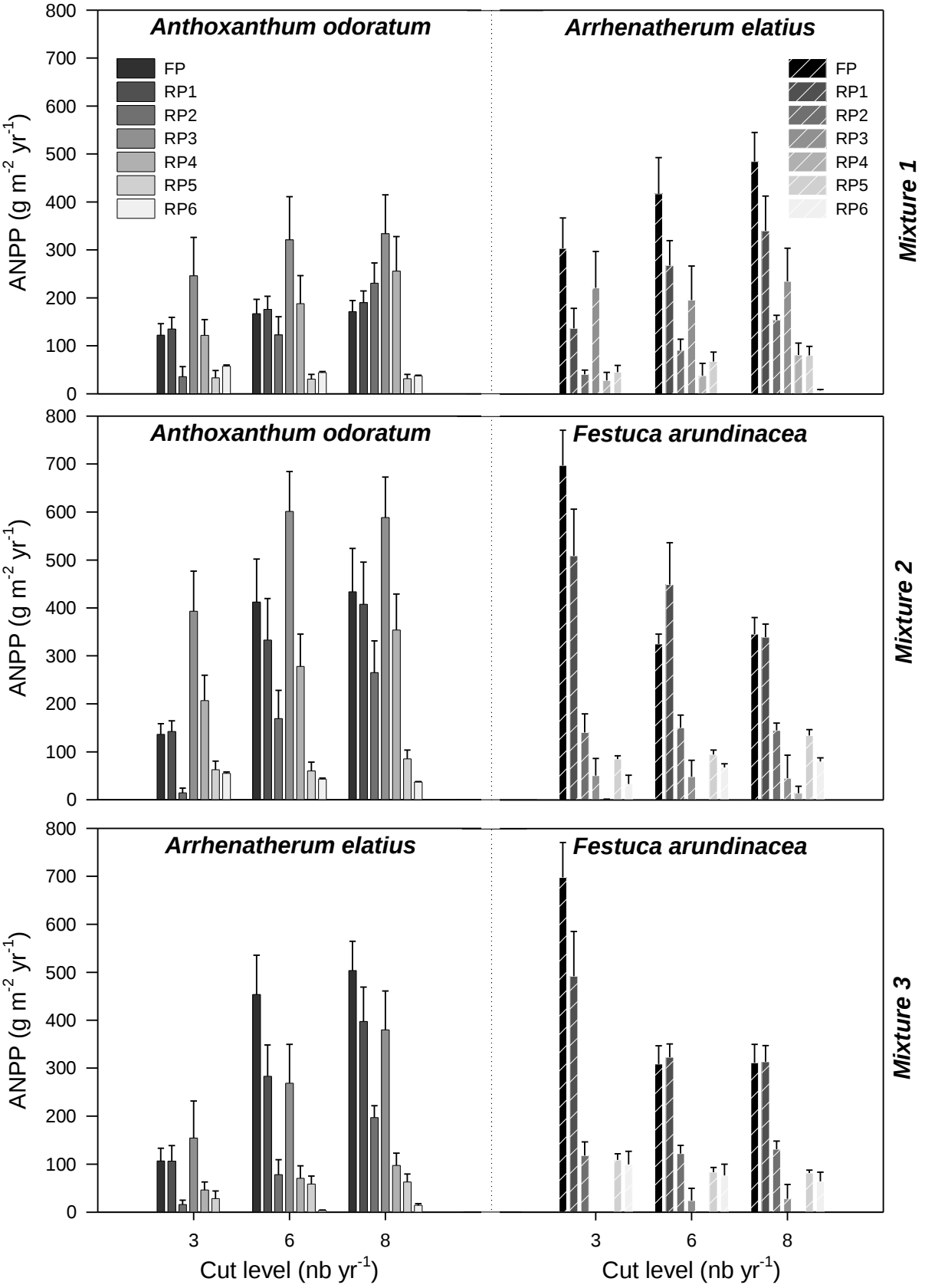

798

799**Figure 7**.

42

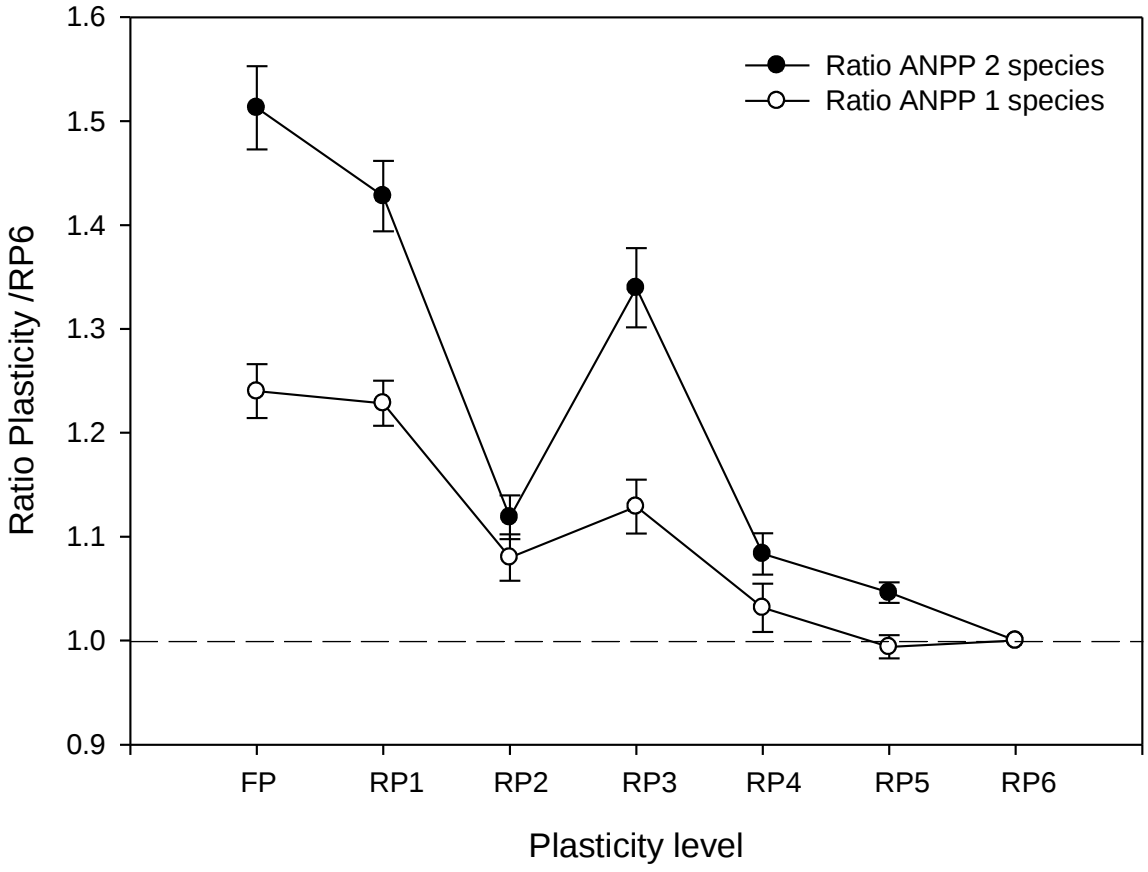

800

801**Figure 8**

43